Spectral dependency of cloud enhanced UV irradiance

Sabburg, J.M * and Parisi, A.V

Faculty of Sciences, University of Southern Queensland, Toowoomba, Australia. 4350

*To whom correspondence should be directed. Email: sabburg@usq.edu.au

Abstract

This paper addresses two questions of primary importance to the solar UV community, 1) “Are cloud induced UV enhancements always wavelength dependent?” and 2) “Are the enhancements greatest in the UVA or UVB wavebands?” The answer to the first question is a definite no, with the conclusion to the second question that most of the enhancements found at this southern hemisphere measurement site are in the UVB waveband. This research is based on the results from a scanning UV spectroradiometer and a colour, all-sky camera over a 19 month period. In both the UVB and UVA wavebands there were cases that showed increasing, decreasing and no spectral dependence towards the shorter and longer wavelengths respectively. This research has found that cases of spectral dependence that decreased with wavelength, tended to correspond to cloud fraction distributed in the outer field of view of the sky camera images for relatively low solar zenith angles. It is speculated that this is most likely due to an increase of scattered UV, compared to cases of increasing trends with wavelength, that would be accounted for by an increase in reflected UV from cloud surfaces in closer proximity to the sun. It also appears that wavelength dependency trends are related to the overall cloud fraction.

Keywords: Spectral; Dependency; Enhanced; Clouds; Ultraviolet; UV

1. Introduction

It has previously been reported, and subsequently reviewed by Parisi et al (2004), that certain configurations of cloud can cause an increase in the ultraviolet (UV) radiation reaching the earth's surface, with respect to an equivalent clear sky scenario (e.g. Bener, 1964; McCormick and Suehrcke, 1990; Mims and Frederick, 1994; Sabburg and Wong, 2000; Sabburg et al., 2001). These reports of UV enhancement due to cloud have been measured in both the UVA (320-400 nm) and UVB (280-320 nm) wavebands. Additionally, the spectral dependency of UV due to cloud, and to some extent cloud enhanced UV, have also been published (e.g. Bais et al., 1993; Seckmeyer et al., 1996; Schwander et al., 2002; Crawford et al., 2003). The reported extent of UV spectral dependency varies, with earlier papers concluding that the scattering of UV radiation by clouds is essentially wavelength independent. Later papers (e.g. Crawford et al., 2003), present both wavelength independent and wavelength dependent (decreasing 'trend') cases, as well as examples of UV enhancement showing an increasing trend with wavelength. The spectral data was presented mainly in the UVA waveband, with some evidence of a continuing trend in the UVB.

There are currently only three published papers specifically relating to the issues of spectral UV enhancement and their wavelength dependency due to cloud (Sabburg et al., 2003, Sabburg and Long, 2004 and Lovengreen et al., 2005). The first two papers discuss preliminary data (collected from two different spectral UV instruments) and posed questions relating to the importance of quality assurance, QA, in relation to measurement methodology, which this current paper partly addresses. The third paper presents data from a multichannel radiometer, effectively a compromise between using broadband

radiometers (e.g. Sabburg and Wong, 2000) and scanning spectral radiometers (e.g. Sabburg et al., 2003). There remains two questions of primary importance to be investigated in this current research, 1) “Are cloud induced UV enhancements always wavelength dependent?” and 2) “Are the enhancements greatest in the UVA or UVB wavebands?”

2. Instrumentation

The measurement site for this research was located at the campus of the University of Southern Queensland (USQ), Toowoomba, Australia (27.5°S, 151.9°E, 693 m altitude). The radiation and environmental monitoring equipment were located atop a 4-storey building with no surrounding hills or trees affecting the field of view (FOV). This site has a relatively unpolluted atmosphere (Parisi and Downs, 2004).

2.1 Spectral Instrument

The solar UV spectrum was recorded from 280 to 400 nm in 0.5 nm increments with a scanning UV spectroradiometer (Bentham Instruments, Reading, UK) based on a double grating monochromator (model DTMc300F) with 2400 lines/mm gratings. This instrument is described in Parisi and Downs (2004). Briefly, it is installed in a container that is weather proof and temperature stabilised (for most of the year). On each day, the spectroradiometer automatically starts scanning at 5:00am Australian Eastern Standard Time (EST), and thereafter every 5 minutes till 7:00pm EST. Each scan takes approximately one minute to initialise and two minutes to complete the scan.

Irradiance and wavelength calibrations were undertaken on 17 March 2003, 10 December 2003, 11 June 2004 and 17 December 2004. The irradiance calibration was

against a 150 W quartz tungsten halogen (QTH) lamp calibrated to the National Physical Laboratory, UK standard and the wavelength calibration against the UV spectral lines of a mercury lamp. On a regular basis between these absolute calibrations, the wavelength calibration was checked and three sets of 150 W QTH lamps were employed to check the irradiance stability. A temporal and temperature correction was required to be applied to the data between 11 June 2004 and 17 December 2004, with no correction required between the other times of the absolute calibrations. After applying the temporal correction, the uncertainty of the spectral UV data was of the order of ±7% (not including ±3% uncertainty in the traceability of the calibration lamp to the UK standard).

2.2 All-Sky Imager and Photodiode

The sky imager and algorithms have been fully described elsewhere (Sabburg and Long, 2004). In summary, the sky imager (Yankee Environmental Systems, YES, TSI-440) was geometrically aligned with the sun so that a shadow band prevented reflection of the sun directly into the digital camera lens. The sky imager was used to capture sky images (160° FOV), automatically every 5 min of daylight, to coincide with the beginning of each spectral scan of the Bentham (described in the last section). Subsequently, digital image processing produced the following parameters which were later used to quantify the sky dome during enhanced UV scans: cloud fraction, cloud uniformity, cloud proximity to the sun and solar obstruction by cloud. The performance of these algorithms has been reported as better than ±76% (Sabburg and Long, 2004), ±76% and ±85% (Long et al., 2005), for cloud fraction, uniformity and obstruction, respectively (not corrected for sun circle or horizon area).

On visual inspection of 788 of the images mentioned in the results section below (where approximately 6 scans were chosen throughout each day), 23% agreement was found for a difference in the cloud fraction (less than or equal to 10%) in the 30° FOV determined by the cloud proximity algorithm and the visual inspection. For cases where this algorithm exceeded the visual inspection by more than 10% (49% of the images), it was found to be due to the "whitening / blooming effects", as described by Long et al. (2005). For cases where the visual inspections exceeded the algorithm by more than 10% (28% of the images), it was found to be due to the misdetection of cirrus cloud fraction. Based on these findings it was decided to perform parallel visual inspections of the images when required.

To overcome previous QA issues, relating to the uncertainty of the sky dome changing significantly during the scanning of the UV spectrum by the spectral instrument (Sabburg and Long, 2004), a photodiode circuit was constructed and the skyward looking photodiode was positioned in the vicinity of the Bentham and all-sky imager. The circuit was based on a '555' timer chip and an 8-bit analogue to digital (A/D) converter. A BASIC program captured the photodiode data (continuously) and stored 5 digital counts (each representing approximately 30 sec), representing the sky light during the duration of the Bentham scans. Digital counts of the incoming sky light (ranging from 0, no skylight, to 50, bright skylight), were tested to an accuracy of ±2% with known light levels. Additionally, on the 17th August and 13th October 2004, the photodiode output was compared to the TSI cloud fraction and solar obstruction algorithms (on the second day the TSI was set to a 10 sec capture time). Although the photodiode output changed by approximately 2% during cases of a cloud fraction change of the order of 15% (for

clouds near the solar disk with the sun not obstructed), the most notable changes of the PD output occurred when the sun became obstructed, or unobstructed, by cloud (with essentially no change in cloud fraction), of the order of 60%. This information was subsequently used to reject spectral scans from the dataset where the digital light counts changed by more than 1% during the 2.5 min period. This approach, of using a PD, ensured that the scanning of the UV waveband (280 to 400 nm in 0.5 nm steps), was 'effectively' equivalent to 240 discrete wavelengths obtained simultaneously, compared to only 4 wavelengths in the UV waveband used in the work of Lovengreen et al. (2005), namely 305, 320, 340 and 380 nm.

3. Results, Analysis and Discussion

The UV and environmental dataset, used in this research, was collected between 30 June 2003 and 25 December 2004 (19 months, 71335 scans). After performing QA on the dataset and rejecting scans where the photodiode indicated that the sky dome conditions had changed, approximately 10% of these scans were available for further analysis.

To address the first of the two questions of primary importance, "Are cloud induced UV enhancements always wavelength dependent?" it was necessary to decide how cases of UV enhancement would be chosen. As the health community is the primary beneficiary of this environmental information, it was decided to focus attention on erythemal UV (UV in the range of 280 to 400 nm, weighted by the erythemal action spectrum (CIE, 1987), specifically the UV index, UVI (WMO, 1994). In other words only the wavelength dependency of scans that were selected as UVI enhanced were considered. To select these cases of UVI enhancements the method of Sabburg and Long

(2004) was chosen (i.e. establishing a clear sky 'envelope' or clear sky UVI versus solar zenith angle, SZA, relationship), with the modification that Total Ozone Mapping Spectrometer (TOMS) ozone data (valid for around 11:15am local time), was used to further categorise the clear sky data into three groups (see below). The TOMS web site states that the latitude dependent error in the data is zero near the equator and -2% to -4% at 50 degrees latitude. The latitude of the current research is 27.5^{o} and so this error is expected to be half this amount. Finally, TOMS aerosol index (AI) data (ranging from -0.48 to 0.9) was used to select the cases of the 'cleanest' (i.e. least aerosol load), clear sky scans (while retaining a statistically significant number of data points for each group), which were finally used to produce the following relatively clean, clear sky envelopes valid for the SZA range of 26 to 70°, with an r^2 of 0.98 to 1.00 (based on a cubic polynomial line-of-best-fit), and an ozone range as indicated:

$$UVI = -4 \times 10^{-6} SZA^3 + 0.0036\, SZA^2 - 0.6157\, SZA + 27.947 \qquad (225 \text{ to } 255 \text{ DU})$$

$$UVI = 8 \times 10^{-5} SZA^3 - 0.0093\, SZA^2 + 0.1027\, SZA + 13.91 \qquad (256 \text{ to } 285 \text{ DU})$$

$$UVI = 9 \times 10^{-5} SZA^3 - 0.0111\, SZA^2 + 0.2334\, SZA + 9.9666 \qquad (286 \text{ to } 345 \text{ DU})$$

The maximum scatter of the data points, centred on the above relationships, was found to be less than ±13%. To ensure that UV enhancements were genuine, and not selected due to either the uncertainty of the Bentham (±7%) or the uncertainty of the clear sky envelopes (±13%), only scans for which the UVI on cloudy days exceeded the corresponding clear sky value by 20% (i.e. 7 + 13%), were chosen. Initially this resulted in 121 scans, but was reduced to 91 scans (with enhancements ranging from 20 to 30%),

over the SZA range of 24 to 70°, after further manual QA was undertaken (e.g. 30 scans did not correspond to actual cloudy skies, but rather due to "whitening / blooming effects").

Table 1 summarises the environmental parameters of cloud fraction (percentage of total 160° FOV, calculated by the standard YES algorithm); cloud uniformity (1 if cloud fraction in the four quadrants of the image were within 20% of the total image cloud fraction, otherwise, 0); cloud proximity to the sun (percentage of cloud in each of four regions: approximately 0 to 30°, 30 to 60°, 60 to 80°, and 80 to 160° FOV, about the solar position within the image) and finally solar obstruction by cloud (1 if cloud blocked the solar disk, else 0, as determined by the standard YES algorithm), for these 91 cases of genuine UVI enhancement. On examination of these cases it was found that on the 10th December 2003, there were 6 cases of continuous UVI enhancement lasting from 1:30 to 1:55pm and a further 5 continual cases lasting from 2:45 to 3:05pm.

Next, for each of the above cases of UVI enhancements, the characteristics of the ratio of each spectrum, to the closest, corresponding, clear sky spectrum (based on differences of ozone amount, < 25 DU, and SZA, < 2°), were examined, resulting in 56 spectral ratios. The cut-off wavelength of each spectrum was chosen when the UV irradiance was less than 5 $mWm^{-2}nm^{-1}$. This avoided inaccurate ratios due to the low photon counts for wavelengths less than the cut-off of the respective spectra. During the testing phase of the above methodology, and by examining the ratio of a number of similar SZA clear-sky, clean scans with those of corresponding model scans (obtained from http://www.acd.ucar.edu/Science/Models/TUV/Interactive_TUV/), it was found that the Bentham produced some scatter in the 0.5 nm UV spectral ratio. This indicates the

possibility that there was a wavelength resolution problem with the Bentham, for at least some of the time during the data collection period. If the spectra obtained from the Bentham (and model) were ideal, there would not be any scatter about a ratio of one.

The consequence of this finding was that 10 spectra were found that had small scatter ($r^2 > 0.80$, for a line-of-best-fit of spectra above 320 nm) (see Figure 1 and Table 2). All 10 spectra had an upward 'turning' trend for decreasing wavelengths less than 310 nm, and as indicated from Table 1, all spectra corresponded to an unobstructed sun. A summary of these 10, and remaining 46 scans, is presented in Table 3. It was not possible to determine if the scatter, mentioned above, was due to equipment, atmospheric or both effects, however, the data does suggest that 64% of the scans were essentially wavelength independent in the UVB, and 66% in the UVA. Of the remaining scans in the UVB (36%), if atmospheric effects are assumed, it is not possible to draw any firm conclusions as to whether the upward or downward trends were due to cloud enhancement or ozone variation, but the data suggests there are more upward than downward trends. In the UVA, there are almost an equal number of scan ratios with positive (29) and negative (27) slopes of the lines-of-best-fit, and it would appear that there are more scans with downward (negative) trends (11), with increasing wavelength, compared to upward (positive) trends (8), i.e. slopes greater than ± 0.0005.

Thus, although this data suggests that the majority of UV enhanced spectra are wavelength independent in the UV (280-400nm), those that are wavelength dependent tend to have a greater number of increasing trends in the UVB, and decreasing trends in the UVA, thus suggesting that on average there are more spectra that are UVB enhanced than UVA enhanced. This suggestion is supported by the average of all 56 UV spectral

enhancements (average UVI ratio of 1.16), for each 0.5 nm wavelength, giving an average of 1.17 for the UVB and 1.14 for the UVA bands respectively.

When the results presented in Table 2 are further examined, it is possible to speculate some criteria for producing cases of upward and downward sloping spectral ratios. It appears that cases of upward slopes are more likely for higher SZA and greater cloud fraction, compared to lower SZA and smaller cloud fraction for downward sloping ratios. When the images corresponding to the 10 spectra are examined, it is also found that cases of downward sloping ratios, with increasing wavelength, tend to have their cloud fraction distributed in the outer FOV of the image, compared to either neutral or upward sloping ratios (Figure 2). This finding was confirmed when visually examining the other 7 downward sloping ratios of the full 56 scan dataset, and will be further investigated in an additional publication. Finally, the cloud fraction data presented in the last column of Table 3 seems to suggest that as the cloud fraction decreases, so does the trend of the slope of the wavelength dependency (progressing from positive, zero to negative slope).

4. Conclusions

This paper has investigated the spectral dependence of the UV spectra that have been cloud enhanced above that of the corresponding clear sky case. In the UVB waveband there were cases that showed increasing, decreasing and no spectral dependence towards the shorter wavelengths. Similarly, for the UVA waveband there was an increasing, decreasing and no spectral dependence towards the longer wavelengths. The data showed that on average there are more spectra that are enhanced in the UVB waveband compared to the spectra that are enhanced in the UVA waveband. This is supported by the findings

from previous broadband data (Sabburg and Wong, 2000), but was not supported from the work of Lovengreen et al. (2005), reported at another southern hemisphere location. Spectra that corresponded to an unobstructed sun possessed a spectral dependence below 310 nm that was higher towards the shorter wavelengths. The cases of spectral dependence that decreased with wavelength tended to have their cloud fraction distributed in the outer FOV of the image when the SZA was usually low.

Due to differences in methodology (e.g. essentially examining cases of an unobstructed sun), and to some extent the type of sky camera employed (e.g. some difficulty in cloud type identification across the solar disk), it was not possible to verify the postulate for maximum cloud induced UVB enhancement, previously proposed by Sabburg and Wong (2000) and more recently by Parisi et. al. (2004). It is also worth noting that Lovengreen et al. (2005) found most of their enhancements when cumuliform clouds were in their dissipation stage and their cloud fringes were crossing over the solar disk.

For this current research, it is speculated that the reason for the cloud distribution, in the outer FOV of the image, causing cases of spectral dependence that decreased with wavelength, is most likely due to an increase of scattered/diffuse UV (which is greater for shorter wavelengths), compared to cases of increasing trends with wavelength, that would be accounted for by an increase in reflected/diffuse UV (equivalent to an increase in direct UV at the sensor), from cloud surfaces (which is greater for longer wavelengths). From the cloud fraction data it can be speculated that as the mix of cloud and clear sky changes (e.g. from mostly cloudy with some blue sky, to some cloud with mostly blue sky), there is a change in the wavelength dependency of the enhanced scans. This could

suggest that the wavelength dependency is not just due to the clouds, but also due to the surrounding Rayleigh scattering of the clear sky (e.g. an apparent neutral dependency could result from UV interactions with the right ‘mix and distribution’ of cloud and sky).

Acknowledgements

The authors acknowledge USQ research assistants Johanna Turner for data preparation and solar proximity performance, Nathan Downs for development of the photodiode circuit, USQ technical staff for general assistance, the ARC for a Discovery Grant enabling purchase of the Bentham Spectroradiometer, and NASA/Goddard Space Flight Center for TOMS ozone and aerosol index data.

References

Bais, A.F., Zerefos, C.S., Meleti, C., Ziomas, I.C. and Tourpali, K., 1993, Spectral measurements of solar UVB radiation and its relations to total Ozone, SO_2, and Clouds, J. Geophys. Res., 98(D3), 5199-5204.

Bener, P. 1964, Investigation on the Influence of Clouds on the Ultraviolet Sky radiation, Contract AF 61(052)-618, Tech. Note 3, Davos-Platz, Switzerland.

CIE (International Commission on Illumination) 1987, A reference action spectrum for ultraviolet induced erythema in human skin, CIE J. 6, 17-22.

Crawford J., Shetter R.E., Lefer B., Cantrell C., Junkermann W., Madronich S. and Calvert J., 2003, Cloud impacts on UV spectral actinic flux observed during the International Photolysis Frequency Measurement and Model Intercomparison (IPMMI), J. Geophys. Res., 108(D14): Art. No. 8545.

Long, C.N., Sabburg, J.M., Calbó, J., and Pagès, D., 2005, Retrieving cloud characteristics from ground-based color all-sky images, submitted to JAOT.

Lovengreen, C., Fuenzalida, H. A., and Videla, L., 2005, On the spectral dependency of UV radiation enhancements due to clouds in Valdivia, Chile (39.8°S), J. Geophys. Res., 110(D14207), doi:10.1029/2004JD005372.

McCormick, P.G. and Suehrcke, H., 1990, Cloud-reflected radiation, Nature, 345, 773.

Mims(III), F.M. and Frederick, J.E., 1994, Cumulus clouds and UV-B, Nature, 371, 291.

Parisi, A.V. and Downs, N., 2004, Cloud Cover and Eye Damaging UV Exposures, Int. J. Biomet., doi:10.1007/s00484-004-0213-7.

Parisi, A. V., Sabburg, J., and Kimlin, M.J., 2004, Scattered and Filtered Solar UV Measurements, in the 'Advances in Global Change Research' series, Kluwer Academic Publishers, Dordrecht.

Sabburg, J. and Long, C.N., 2004, Improved sky imaging for studies of enhanced UV irradiance, Atmos. Chem. Phys., 4, 2543-2552.

Sabburg, J.M., Parisi, A.V. and Kimlin, M.G., 2003, Enhanced spectral UV irradiance: a 1 year preliminary study, Atmos. Res., 66(4), 261-272.

Sabburg, J., Parisi, A.V. and Wong, J., 2001, Effect of cloud on UVA and exposure to humans, Photochem. Photobiol., 74, 412-416.

Sabburg, J. and Wong, J., 2000, The effect of clouds on enhancing UVB irradiance at the earth's surface: a one year study, Geophys. Res. Lett., 27 (20), 3337-3340.

Schwander, H., Koepke, P., Kaifel, A. and Seckmeyer, G., 2002, Modification of spectral UV irradiance by clouds, J. Geophys. Res., 107(D16), 10.1029/2001JD00129727.

Seckmeyer, G., Erb, R. and Albold, A., 1996, Transmittance of a cloud is wavelength dependent in the UV range, Geophys. Res. Lett., 23(20), 2753-2755.

WMO, 1994, Report of the WMO Meeting of Experts on UV-B Measurements, Data Quality and Standardization of UV Indices, Les Diablerets, Switzerland, 25-28 July 1994, WMO/TD-NO, 625.

Table 1 – Summary of four environmental parameters corresponding to UVI enhancements (average and range), and for the maximum case of UVI enhancement (equal to 1.25, see Figure 2(b)):

	Cloud Fraction (%)		**Cloud Uniformity (Yes:1/No:0)**		**Solar Proximity (% for each region)**		**Solar Obstruction (Yes:1/No:0)**	
All UVI enhancements					41.7 17.6 11.8	0-95 0-85 0-97		
(Average/Range)	25	2-97	0.05	0-1	10.7	0-100	0	0
Maximum UVI enhancement	59		0		40/40/40/50*		0	

***** Based on a visual observation

Table 2 – Summary of four physical properties relating to the 10 scans that displayed cloud enhanced UV (the grey region separates the curves with increasing slopes of the line-of-best-fit, with those of decreasing slopes):

Curves in Figure 1	**Cloud Fraction (%)**	**Cloud Uniformity (Yes:1/No:0)**	**Slope of fitted-line for $\lambda > 320$ nm**	**SZA (°)**
(a) 1	73	0	0.0019	53
(a) 2	56	1	0.0019	61
(a) 3	78	0	0.0014	50
(b) 1	67	1	0.0005	62
(b) 2	32	0	-0.0005	29
(b) 3	29	0	-0.0003	28
(b) 4	8	0	-0.0004	35
(c) 1	11	0	-0.0009	28
(c) 2	6	0	-0.0009	29
(c) 3	8	0	-0.0009	29

Table 3 – Summary of curvature, slopes and cloud fraction of all 56 scans:

	Tendency of curve with decreasing wavelength less than 320 nm UP / NEUTRAL / DOWN	**Slope of fitted-line with increasing wavelength from 320 nm**	**Cloud fraction (%) UP / NEUTRAL / DOWN**
Range	18 / 36 / 2	-0.0009 to 0.0026	(29-97) / (2-78) / (2-12)
Average	Neutral	0.0003	58 / 19 / 8

FIGURE CAPTIONS

Figure 1: The 10 spectra that had a scatter corresponding to an $r^2 > 0.80$, for spectra above 320 nm, showing trends with increasing wavelength, (a) sloping up, (b) level, (c) down. These corresponded to the lines-of-best-fit to the data.

Figure 2: Example images from the TSI corresponding to, (a) an upward sloping ratio (1:30pm, 21st July, 2004), (b) horizontal ratio (also highest UVI, 9:30am, 15th December, 2003), and (c) a downward sloping ratio (11:45am, 21st September, 2004).

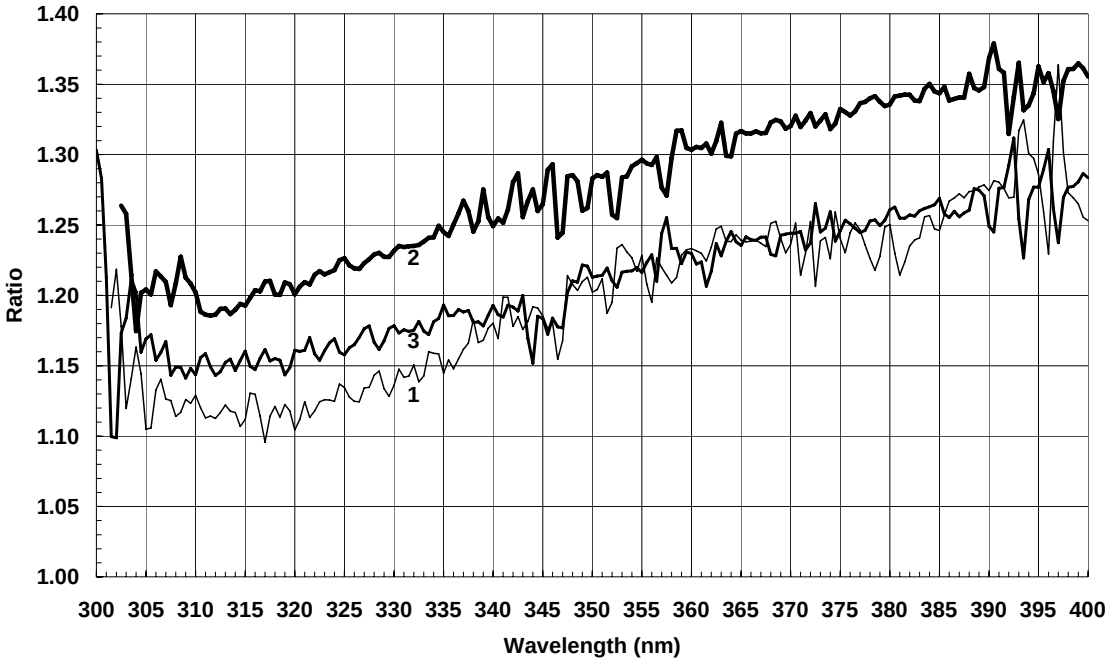

(a)

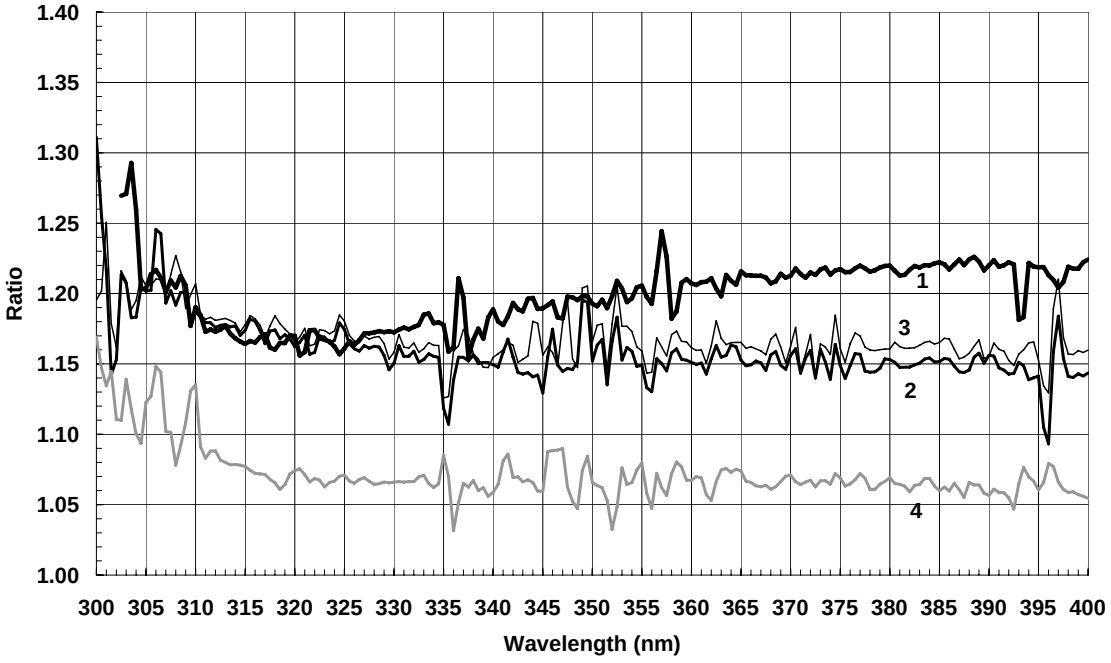

(b)

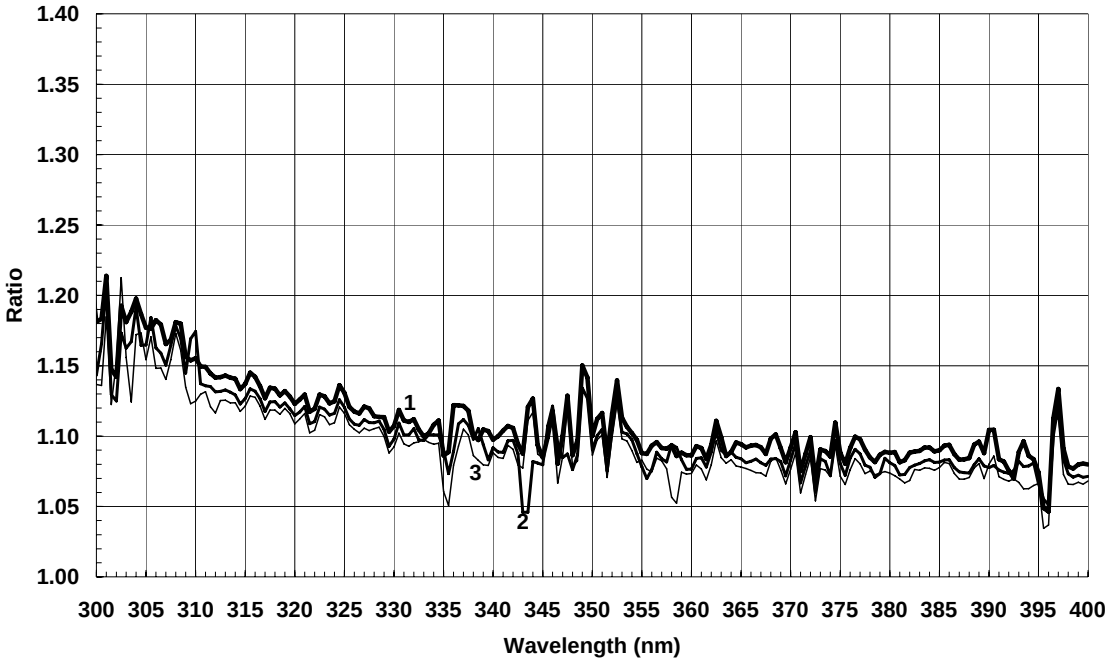
1.40
1.35
1.30
1.25
1.20
1.15
1.10
1.05
1.00
Ratio
1
2
3
300 305 310 315 320 325 330 335 340 345 350 355 360 365 370 375 380 385 390 395 400
Wavelength (nm)

(c)

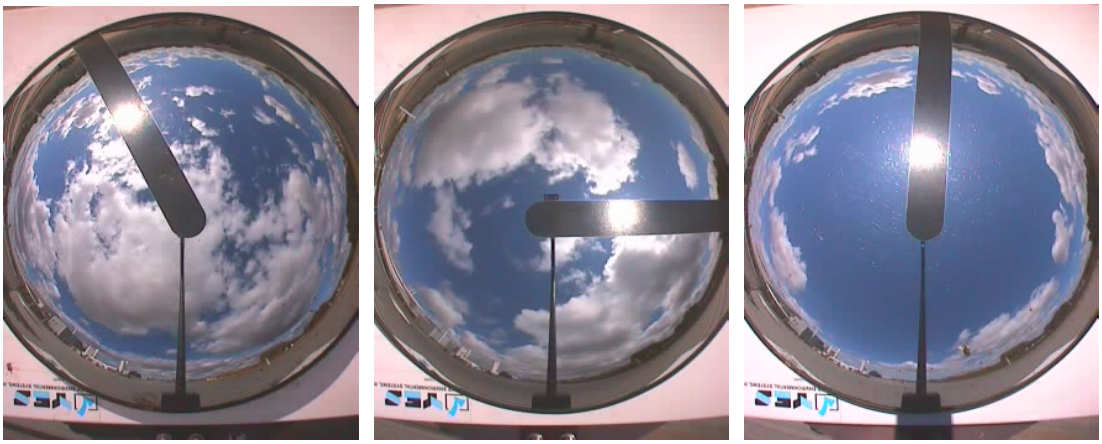

(a) (b) (c)